

An Acoustic On-Chip Goniometer for Room Temperature Macromolecular Crystallography

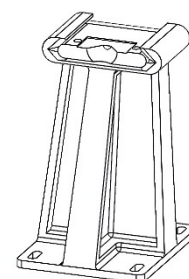
C. G. Burton,^a D. Axford,^b A.M.J. Edwards,^c R. Gildea,^b R.H. Morris,^c M. I. Newton,^c A.M.Orville,^d M.Prince,^a P.D.Topham,^a and P.D.Docker,^{b†}

- a. Aston Institute of Material Research, Aston University, Birmingham B4 7ET, England
 - b. Diamond Light Source, Harwell Science and Innovation Campus, Oxfordshire OX11 0DE, England
 - c. School of Science and Technology, Nottingham Trent University, Clifton Lane, Nottingham, NG11 8NS, England
 - d. Research Complex at Harwell and Diamond Light Source, Harwell Science and Innovation Campus, Oxfordshire OX11 0DE, England
- † Corresponding author

Electronic Supporting Information:

ESI 1. Kinematic Mount CAD Geometry

A geometry file of the mount used to position surface acoustic wave chips. The file may be opened with any IGES capable viewer. Thumbnail image:



ESI 2. Diffraction Image

An image showing the quality of diffraction achieved during crystal actuation and imaging

ESI 3. Actuation Video

A video demonstrating the actuation of thermolysin crystals. The second half of the video is enhanced with both zoom and contrast improvements. This is useful as protein crystals typically have a refractive index very close to that of water. During the early stage of the video it is possible to spot crystals using their birefringent properties causing a slight shift in the colour spectrum. The crystals may be recognised as rod shapes of varying length.

ESI 4. Infrared Video

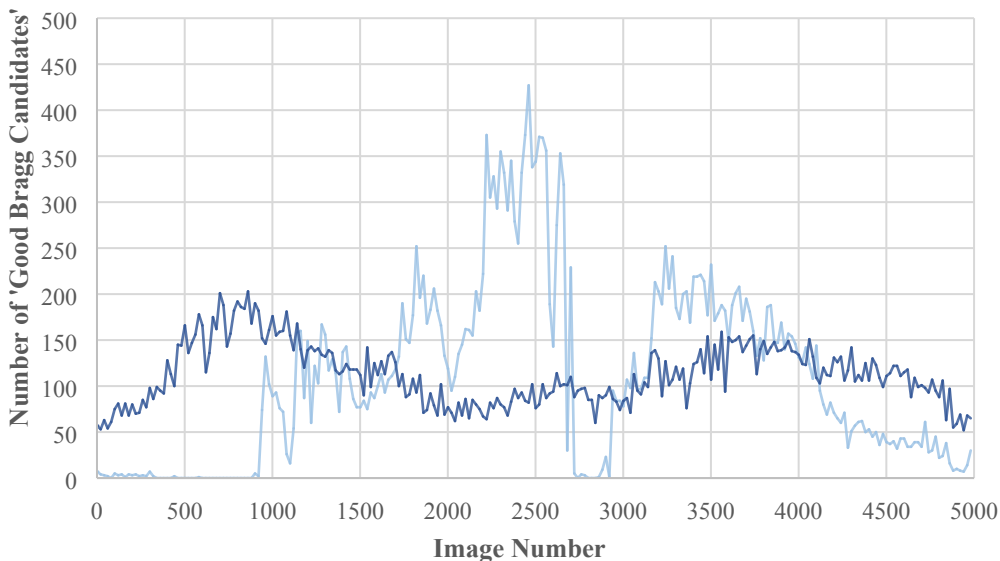
A video depicting infrared imaging of crystals experiencing intermittent surface acoustic wave power. The transducer (power source) and the drop have been labelled for clarity.

ESI 5. Rotation Animation

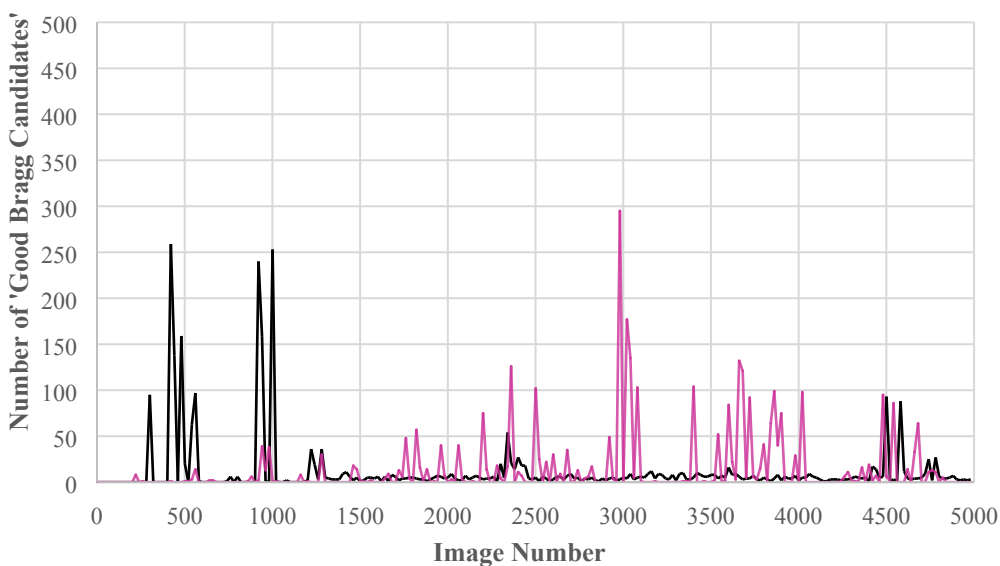
An animation showing the rotation motion of a thermolysin crystal during the dataset used to create the structure submitted to the Protein Data Bank (PDB ID:508N, releasing 9th August 2017).

ESI 6. Plots showing the Bragg diffraction spot counts at the central and edge regions of an acoustically excited drop.

In the experiment as described, the location of crystals within the droplet was effected by SAW actuation. A vortex was induced by SAW which forced the crystals to spin around the droplet. The experimental arrangement did allow fine positioning of the device and droplet with respect to the beam, however the method allowed a multitude of crystals to be present in a drop rather than the specific targeting of a crystal. For data collection the beam was located the beam at the centre of the droplet and the vortex, since a crystal tended to remain in the beam, rotating. When the beam was located towards the edge of a drop, it was apparent that crystals were orbiting in and out of the beam. The plots below illustrate the difference in data collection rates, where Bragg spots were defined by the software DISTL implemented in the DIALS package.¹



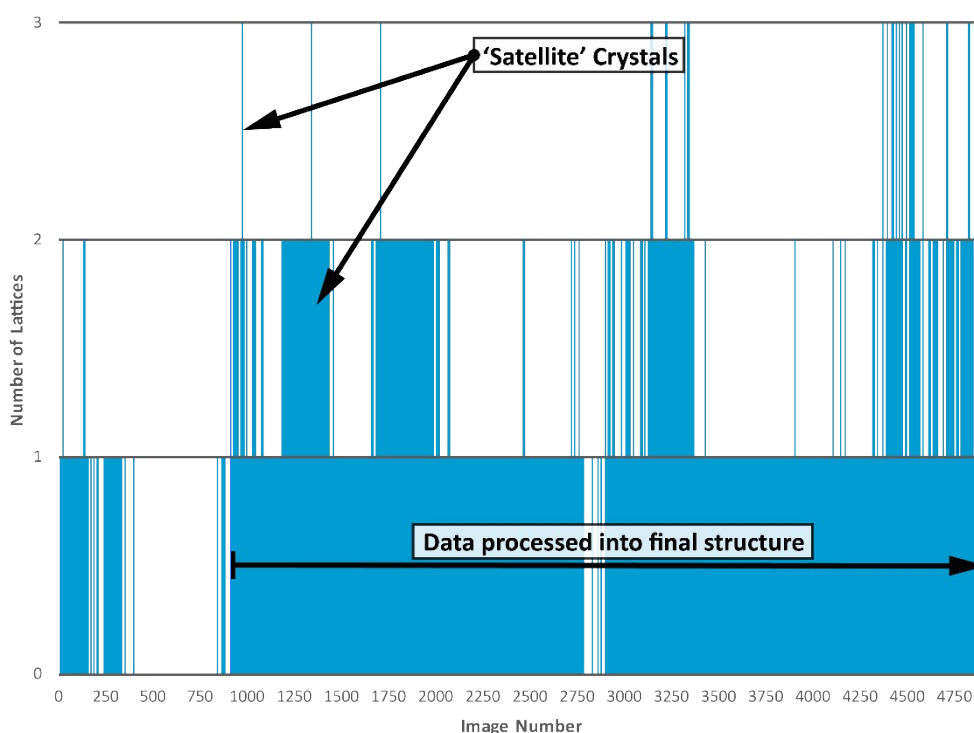
Bragg candidate spots found per image during two separate collection runs from the centre of a drop, during approximately 50 seconds of data collection



Bragg spots found per image during two separate collection runs from the edge of a drop, during 50 seconds of data collection

ESI 7. Plot showing the frequency of multi crystal diffraction in the beam and the ability to define and separate those lattices.

Historically, deconvolving diffraction from multiple crystals has been a problem, however recent progress in crystallographic analysis, including in the DIALS framework we were using has made this much easier. Gildea et al, 2014² describe how up to 10 single crystal lattices can be identified and separated from diffraction data covering only small volumes of reciprocal space. During the data collection we found that there was a tendency for a single crystal lattice to dominate (at centre of vortex) with other lattices only appearing transiently as they orbited around the centre of the vortex. This effect did not significantly hinder identification and measurement of useful diffraction data in this experiment, indeed Figure 4 (the scatter plot of Euler angles) confirms a single lattice can be identified and tracked. A plot is included below and has also been added to the ESI, with an in text reference, showing lattices found for each diffraction image for the data run used for the deposited structure.



- (1) Zhang, Z.; Sauter, N. K.; Van Den Bedem, H.; Snell, G.; Deacon, A. M. Automated Diffraction Image Analysis and Spot Searching for High-Throughput Crystal Screening. *J. Appl. Crystallogr.* **2006**, *39* (1), 112–119 DOI: 10.1107/S0021889805040677.
- (2) Gildea, R. J.; Waterman, D. G.; Parkhurst, J. M.; Axford, D.; Sutton, G.; Stuart, D. I.; Sauter, N. K.; Evans, G.; Winter, G. New Methods for Indexing Multi-Lattice Diffraction Data. *Acta Crystallogr. Sect. D Biol. Crystallogr.* **2014**, *70* (10), 2652–2666 DOI: 10.1107/S1399004714017039.